

# Asymmetric total synthesis of benzenoid cephalotane-type diterpenoids through a cascade C(sp<sup>2</sup>) & C(sp<sup>3</sup>)-H activation

Received: 16 December 2024

Accepted: 6 May 2025

Published online: 20 May 2025

Check for updates

Xiangxin Li, Zhaoxu Lu, Shaocong Liu, Mengyao Sun, Shengfu Duan &amp; Zhixiang Xie

Cephalotane diterpenoids, featuring unique and complicated carbon skeletons and remarkable antitumor activities from the *Cephalotaxus* genus, have been gaining increasing attention. Herein, we report the asymmetric and divergent total synthesis of benzenoid cephalotane-type diterpenoids containing the identical 6/6/6/5 tetracyclic and the bridged  $\delta$ -lactone skeleton with different oxidation states. A cascade of C(sp<sup>2</sup>) and C(sp<sup>3</sup>)-H activation has been developed to efficiently prepare the characteristic and synthetically challenging 6/6/6/5 tetracyclic skeleton through a pivotal palladium/NBE-cocatalyzed process. The feature of this strategy is the construction of three C-C bonds (two C(sp<sup>2</sup>)-C(sp<sup>3</sup>) bonds and one C(sp<sup>3</sup>)-C(sp<sup>3</sup>) bond) and the formation of two cycles with two chiral centers in a single step. The application of this method for the rapid assembly of the skeleton of benzenoid cephalotane-type diterpenoids is demonstrated through the concise and asymmetric total synthesis of cephanolides A-D (**1-4**) and ceforalide B (**5**) via late-stage modification.

Cephalotane diterpenoids, characterized by unique and intricate carbon skeletons and notable antitumor activities, are distinctive compounds of the *Cephalotaxus* genus, comprising over 110 members<sup>1-6</sup>. Benzenoid cephalotane-type diterpenoids are a relatively novel subtype (Fig. 1a), as the isolation, named cephanolides A-D, was reported in 2017 by Yue and co-workers<sup>7</sup>. Up to now, eight other benzenoid cephalotane-type diterpenoids have been isolated from the seeds of *Cephalotaxus fortunei* var. *Alpina* by the same group<sup>2,6</sup>. Structurally, these molecules have a unique 6/6/6/5 tetracyclic core embedded with a bridged  $\delta$ -lactone, containing<sup>5-7</sup> contiguous stereogenic centers (Fig. 1b). In addition, the oxidation states of benzenoid cephalotane-type diterpenoids exhibit diversity at the C3, C7, C10, C13, and C20 positions.

Due to their intricate and diverse structures, as well as their potential biological activities, benzenoid cephalotane-type diterpenoids have garnered significant attention from synthetic chemists (Fig. 1c). Synthetic studies have been comprehensively reviewed by

Yue and co-workers<sup>8</sup>. The total synthesis of benzenoid cephalotane-type diterpenoids was reported by Zhao and co-workers<sup>9</sup>. They utilized a palladium-catalyzed cascade cyclization reaction to forge the 6-5-6 *cis*-fused tricyclic core and successfully achieved the synthesis of ( $\pm$ )-cephanolide B and C (**2-3**) in 2018. The asymmetric total synthesis of cephanolide A (**1**) was achieved by Gao and co-workers through an intramolecular Prins cyclization, followed by a cation-mediated etherification/Friedel-Crafts cyclization<sup>10</sup>. Later, they also realized the asymmetric total synthesis of cephanolide B (**2**) using the same strategy<sup>11</sup>. Guided by chemical network analysis, Sarpong and co-workers realized the divergent total synthesis of ( $\pm$ )-cephanolides A-D (**1-4**) by taking advantage of an intramolecular Diels-Alder cycloaddition to forge the core skeleton<sup>12</sup>. One year later, they optimized the synthesis method to achieve the synthesis of ( $\pm$ )-cephanolides A-D (**1-4**), ceforalides C-D, and F-G<sup>13</sup>. The asymmetric total synthesis of cephanolides A-B (**1-2**) was completed by Cai and co-workers via an inverse-electron-demand Diels-Alder reaction<sup>14</sup>. Using a tandem

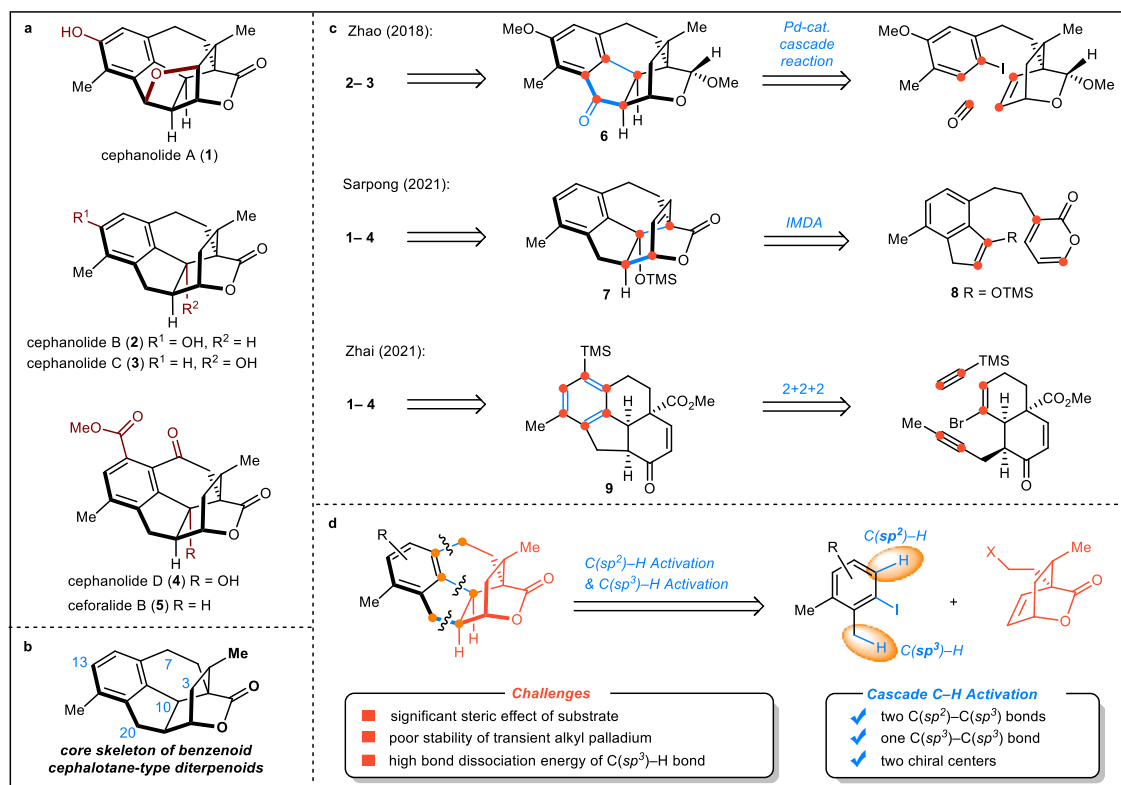


**Fig. 1 | Background and reaction design.** **a** Selected examples of benzenoid cephalotane-type diterpenoids. **b** Core skeleton of benzenoid cephalotane-type diterpenoids. **c** Representative cases of total syntheses of benzenoid cephalotane-type diterpenoids. **d** Our convergent synthetic strategy.

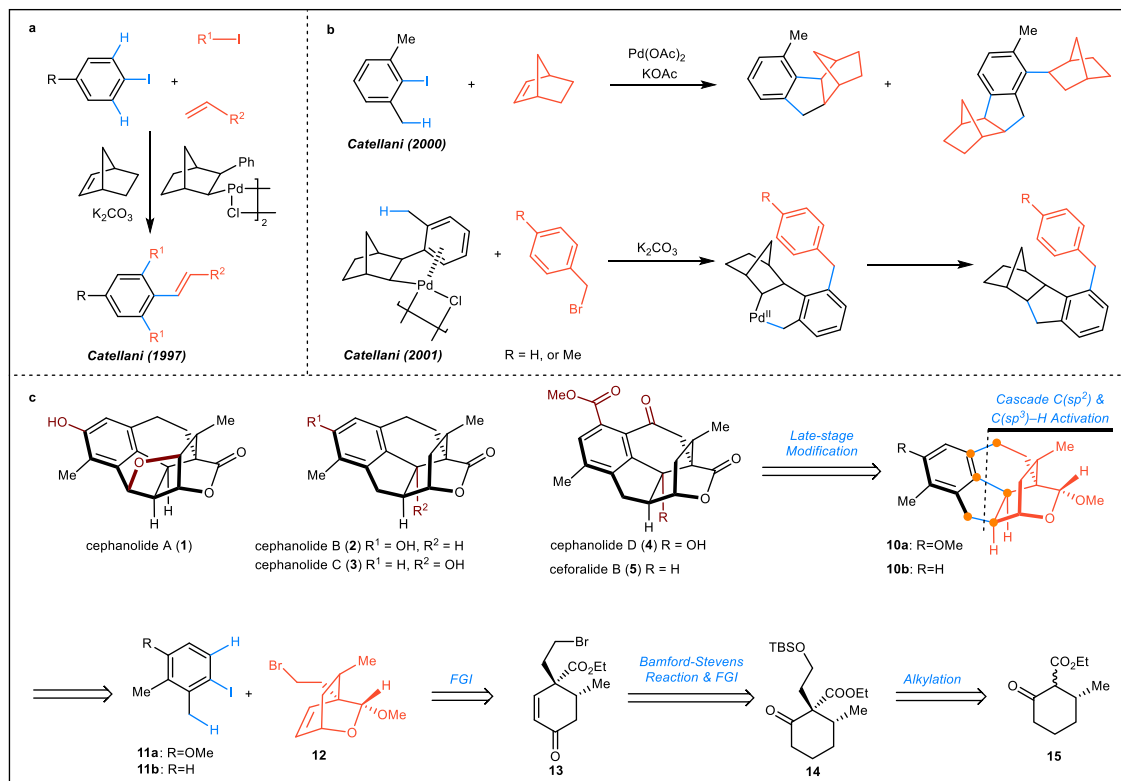


**Fig. 2 |  $\text{C}(\text{sp}^2)$  &  $\text{C}(\text{sp}^3)\text{-H}$  activation and retrosynthetic analysis of benzenoid cephalotane-type diterpenoids.** **a** Catellani reported a  $\text{C}(\text{sp}^2)\text{-H}$  bond activation reaction. **b** Catellani reported  $\text{C}(\text{sp}^3)\text{-H}$  bond activation reaction. **c** Retrosynthetic

analysis of benzenoid cephalotane-type diterpenoids. FGI functional group interconversion.

intramolecular Pauson-Khand reaction, 6 $\pi$ -electrocyclization reaction, and oxidative aromatization strategy, ( $\pm$ )-cephanolide B (**2**) and cephanolides B-D (**2-4**) were synthesized by Yang's group<sup>15</sup> and Hu's group<sup>16</sup>, respectively. The asymmetric total synthesis of cephanolides A-D (**1-4**) was reported by Zhai and co-workers via a palladium-catalyzed formal bimolecular [2 + 2 + 2] cycloaddition reaction<sup>17</sup>. In addition, other subgroups of *cephalotaxus* diterpenoids have also been extensively studied<sup>8,18-21</sup>.

A challenging synthetic strategy was envisioned wherein the core skeleton of benzenoid cephalotane-type diterpenoids was

disconnected into two intermediates, such as aryl iodide and bridged  $\delta$ -lactone, by breaking three C-C bonds (Fig. 1d). The strategy has its own unique challenges, which involves a cascade C(sp<sup>2</sup>) & C(sp<sup>3</sup>)-H activation and the precise construction of three C-C bonds and two chiral centers. The cascade C(sp<sup>2</sup>) & C(sp<sup>3</sup>)-H activation strategy, if effective, might also prove valuable for total syntheses of a variety of natural products featuring the 6/6/6/5 tetracyclic skeleton.

As widely acknowledged, C-H bond activation has been regarded as the Holy Grail of organic chemistry and the ideal strategy of organic synthesis<sup>22-25</sup>. The selective cleavage of C-H bonds enables the efficient formation of other functional groups or novel chemical bonds, thereby significantly enhancing the synthesis efficiency and atom economy for natural product syntheses<sup>26-31</sup>. The Catellani reaction, renowned as a classical C(sp<sup>2</sup>)-H bond activation reaction, was discovered by Catellani<sup>32</sup> in 1997 (Fig. 2a). The reaction has been expanded by Catellani<sup>33</sup>, Lautens<sup>34-36</sup>, Dong<sup>37-39</sup>, and others<sup>40,41</sup> as a very powerful tool used in the synthesis of complex molecules featuring polysubstituted arenes. To date, numerous synthetic chemists have employed the Catellani reaction to accomplish the sophisticated synthesis of natural products<sup>42-54</sup>.

Compared the C(sp<sup>2</sup>)-H bond activation in the Catellani reaction, the activation of C(sp<sup>3</sup>)-H bonds has been less explored, particularly in the formation of C(sp<sup>3</sup>)-C(sp<sup>3</sup>) bonds through the activation of a C(sp<sup>3</sup>)-H by transient alkylpalladium<sup>55,56</sup>. (Fig. 2b) The main challenges lie in the C(sp<sup>3</sup>)-H bond possessing high bond dissociation energy and a lack of stabilizing orbital interactions with the metal center<sup>57,58</sup>. Herein, we present the realization of the rare cascade C(sp<sup>2</sup>)-H and C(sp<sup>3</sup>)-H activation via Pd(O)/NBE-cocatalysis, resulting in the concise and convergent synthesis of cephanolides A-D (**1-4**) and ceforalide B (**5**).

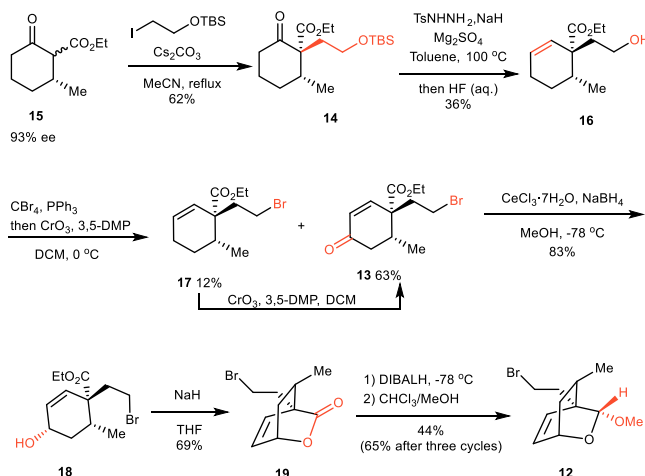


**Fig. 3 | Synthesis of key intermediate 12.** 3, 5-DMP: 3,5-dimethylpyrazole.

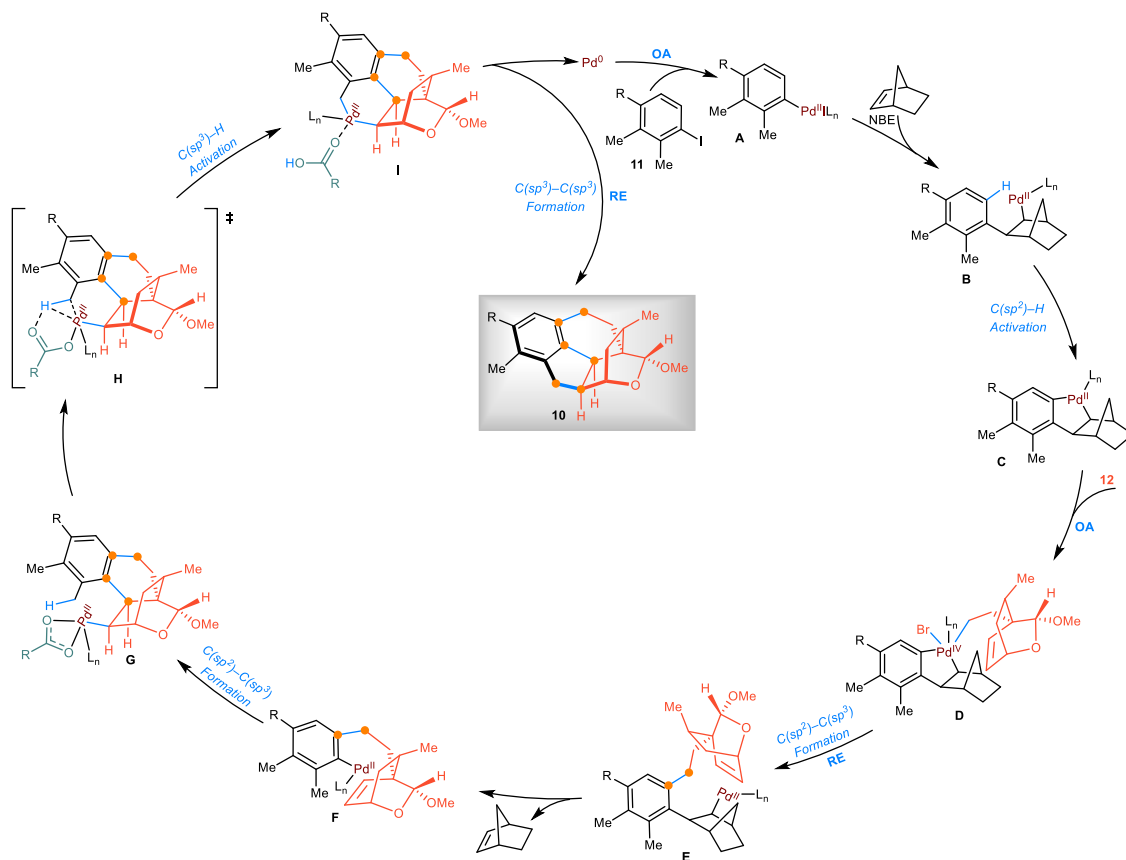


**Fig. 4 | Proposed mechanism of cascade C(sp<sup>2</sup>) & C(sp<sup>3</sup>)-H activation.** Arylpalladium (A), intermediate (B), aryl-norbornyl-palladacycle (ANP) (C), Pd(IV) intermediate (D), ortho-alkylated intermediate (E), intermediate (F), transient secondary alkylpalladium (G), transient secondary alkylpalladium (H), six-membered palladacycle (I). OA oxidative addition, RE reductive elimination.

The key cascade  $C(sp^2)$ -H and  $C(sp^3)$ -H activation reaction, featuring the construction of three C-C bonds and two chiral centers accurately, allows access to the core skeleton of benzenoid cephalotane-type diterpenoids, such as **10a** and **10b**, from iodo-benzene derivatives (**11a** and **11b**) and alkyl bromide **12** in one step, respectively (Fig. 2c). Thus, the asymmetric total synthesis of benzenoid cephalotane-type diterpenoids could be easily achieved from **10a** and **10b** via a late-stage modification strategy. The alkyl bromide **12** could be constructed from cyclohexanone **13** via reduction and acetalization. Ketone **13** could be prepared by Bamford-Stevens reaction and subsequent functional group interconversion (FGI) from compound **14**, which could be derived from a known compound **15**<sup>59</sup>.

## Results

Our synthesis work commenced with the preparation of C10 unit acetal **12** from the known chiral compound **15**, which was prepared from cyclohexanone in one step with 75% yield and 93% ee<sup>59</sup> (Fig. 3).

The alkylation of compound **15** with a 2-iodoethanol derivative, conditions previously reported by Zhu<sup>60</sup>, furnished compound **14** as a single diastereomer in up to 62% yield on decagram scale. Exposure of **14** to a one-pot olefin formation<sup>61</sup>/deprotection protocol yielded alcohol **16**, which was then subsequently treated with  $CBR_4$  and  $PPh_3$ ,

followed by  $CrO_3$  and 3,5-DMP to obtain cyclohexanone **13**, along with a small amount of compound **17**. Noteworthy, olefin **17** can convert to cyclohexanone **13** through the same oxidation. Cyclohexanone **13** was reduced by  $CeCl_3 \cdot 7H_2O$  and  $NaBH_4$  to produce allyl alcohol **18**, which was transformed to lactone **19** in the presence of  $NaH$ . Finally, to avoid potential stereoselectivity issues during the cascade reaction, lactone **19** was further converted to acetal **12**, which has been proven effective in precisely constructing stereochemistry at the C1 and C10 positions by Zhao<sup>8</sup>, Yang<sup>14</sup>, and Hu<sup>15</sup>. Thus, lactone **19** was reduced by DIBALH to produce the corresponding aldehyde, which was then directly transformed into acetal **12** in the presence of chloroform and methanol to prevent the formation of the dimethyl acetal byproduct.

## Cascade $C(sp^2)$ & $C(sp^3)$ -H activation

With acetal **12** in hand, our focus turned toward the pivotal palladium/NBE-cocatalyzed cascade  $C(sp^2)$  &  $C(sp^3)$ -H activation for the assembly of the tetracyclic skeleton. First, the reaction mechanism was proposed<sup>62–64</sup> (Fig. 4). Iodobenzene derivative **11** and  $Pd(0)$  undergo oxidative addition to generate arylpalladium **A**, which is followed by insertion into NBE to produce intermediate **B**. Subsequently,  $C(sp^2)$ -H activation generates aryl-norbornyl-palladacycle (ANP) **C**. Next, the ANP **C** undergoes oxidative addition with compound **12** to produce

**Table 1 | Investigation of the palladium-mediated cascade  $C(sp^2)$  &  $C(sp^3)$ -H activation<sup>a</sup>**

Entry	[Pd]	Solvent	Additive (Delay before addition & Addition time)	Result <sup>b</sup>
1 <sup>c</sup>	20 mol% $Pd(OAc)_2$	DMF	-	<b>20a</b> (43%), <b>21</b> (24%)
2	20 mol% $Pd(OAc)_2$	DMF	-	<b>10a/20a</b> (46%, 1/4.9), <b>21</b> (24%)
3 <sup>d</sup>	20 mol% $Pd(OAc)_2$	DMF	-	<b>10a/20a</b> (45%, 1/5), <b>21</b> (23%)
4	20 mol% $Pd(OAc)_2$	DMF	0.4 equiv. KOiPr	<b>10a/20a</b> (34%, 1/4.6), <b>21</b> (23%), <b>22</b> (21%)
5	20 mol% $PdCl_2$	DMF	0.4 equiv. KOiPr	<b>10a/20a</b> (46%, 1/5), <b>22</b> (21%)
6	20 mol% $PdCl_2$	DMF	1.5 equiv. KOiPr (60 s & 30 s)	<b>10a/20a</b> (29%, 4.1/1), <b>22</b> (68%)
7	20 mol% $PdCl_2$	DMF	1.8 equiv. KOiPr (60 s & 30 s)	<b>10a/20a</b> (27%, 4.4/1), <b>22</b> (73%)
8	20 mol% $PdCl_2$	DMF	2.0 equiv. KOiPr (60 s & 30 s)	<b>10a/20a</b> (23%, 4.4/1), <b>22</b> (75%)
9	20 mol% $PdCl_2$	DMF	1.8 equiv. KOiPr (50 s & 30 s)	<b>10a/20a</b> (24%, 4.5/1), <b>22</b> (72%)
10	20 mol% $PdCl_2$	DMF	1.8 equiv. KOiPr (70 s & 30 s)	<b>10a/20a</b> (26%, 3.8/1), <b>22</b> (72%)
11 <sup>e</sup>	20 mol% $PdCl_2$	DMF	1.8 equiv. KOiPr (60 s & 30 s)	<b>10a/20a</b> (17%, 2.4/1), <b>22</b> (79%)
12 <sup>f</sup>	20 mol% $PdCl_2$	DMF	1.8 equiv. KOiPr (60 s & 30 s)	<b>10a/20a</b> (12%, 2.2/1), <b>22</b> (85%)
13 <sup>g</sup>	20 mol% $PdCl_2$	DMF	1.8 equiv. KOiPr (60 s & 30 s)	<b>10a/20a</b> (10%, 2.2/1), <b>22</b> (86%)
14 <sup>h</sup>	20 mol% $PdCl_2$	DMF	1.8 equiv. KOiPr (60 s & 30 s)	<b>22</b> (95%)
15	20 mol% $PdCl_2$	PhMe	1.8 equiv. KOiPr (60 s & 30 s)	not detected
16	20 mol% $PdCl_2$	PhCN	1.8 equiv. KOiPr (60 s & 30 s)	<b>10a/20a</b> (<10%, 1/5.6), <b>22</b> (33%)
17	20 mol% $PdCl_2$	<i>t</i> -BuCN	1.8 equiv. KOiPr (60 s & 30 s)	<b>10a/20a</b> (<10%, 1.5/1), <b>22</b> (56%)
18	20 mol% $PdCl_2$	DMF/PhMe = 1/1	1.8 equiv. KOiPr (60 s & 30 s)	<b>10a/20a</b> (49%, 10/1), <b>22</b> (61%)
19	20 mol% $PdCl_2$	DMF/PhMe = 1/2	1.8 equiv. KOiPr (60 s & 30 s)	<b>10a/20a</b> (28%, 16/1), <b>22</b> (73%)
20 <sup>i</sup>	20 mol% $PdCl_2$	DMF/PhMe = 1/1	1.8 equiv. KOiPr (120 s & 50 s)	<b>10a</b> (42%), <b>22</b> (64%)
21	20 mol% $PdCl_2$	DMF/PhMe = 1/1	1.8 equiv. KOiPr (80 s & 30 s)	<b>10b/20b</b> (38%, 10/1), <b>22</b> (67%)

<sup>a</sup>Reaction conditions: **11a** or **11b** (0.05 mmol), **12** (0.075 mmol), [Pd]: tri(2-furyl)phosphine (ligand) = 1:2, NBE (0.2 mmol), and  $Cs_2CO_3$  (0.15 mmol) in solvent (1.2 mL) under an argon atmosphere, 120 °C.

<sup>b</sup>The ratio of **10a** and **20a** was determined by <sup>1</sup>H NMR spectroscopy. The yields of **10a-b** and **20a-b** were calculated against **11a-b**. The yields of **21-22** were calculated against **12**. Isolated yield.

<sup>c</sup>The reaction was conducted in 110 °C.

<sup>d</sup>The reaction was conducted in 130 °C.

<sup>e</sup>Triphenylphosphine as ligand.

<sup>f</sup>Tris(4-methoxyphenyl)phosphine as ligand.

<sup>g</sup>Tris[4-(trifluoromethyl)phenyl]phosphine as ligand.

<sup>h</sup>1,3-Bis(diphenylphosphino)propane as ligand.

<sup>i</sup>0.9 mmol **11a**.

Pd(IV) intermediate **D**, followed by reductive elimination to obtain ortho-alkylated intermediate **E**. Then, the  $\beta$ -carbon elimination of intermediate **E** leads to the formation of intermediate **F**, which subsequently proceeds through an intramolecular migratory insertion to generate the crucial transient secondary alkylpalladium **G**. In the last stage, transient secondary alkylpalladium **H** undergoes a concerted metalation deprotonation (CMD) process to yield six-membered palladacycle **I**, and subsequent reductive elimination to provide the desired **10**.

As shown in Table 1, an initial attempt with tri(2-furyl)phosphine as the ligand and  $\text{Cs}_2\text{CO}_3$  as the base was conducted at 110 °C. The  $\text{C}(\text{sp}^2)\text{-H}$  activation product **20a** was obtained in 43% yield along with the nucleophilic substitution byproduct **21**, but the cascade  $\text{C}(\text{sp}^2)$  &  $\text{C}(\text{sp}^3)\text{-H}$  activation product was not observed (entry 1). When the reaction temperature was raised to 120 °C, the desired compound **10a** was obtained, albeit accompanied by a significant amount of compounds **20a** and **21** (entry 2). Further increasing the reaction temperature did not achieve a better result (entry 3). The yield of byproduct **21** indicates that nucleophilic substitution by acetate anions is fast, rendering them unable to participate in the CMD

process of crucial  $\text{C}(\text{sp}^3)\text{-H}$  activation. Therefore, to inhibit nucleophilic substitution and promote the CMD process, KO<sub>2</sub>Piv, which has a larger steric effect, was added. However, the yield of **10a/20a** (1/4.6) decreased to 34%, while the yield of **21/22** increased to 44% (entry 4). This result may indicate that the nucleophilic substitution of acetal **12** with carboxylate is much faster than the oxidative addition of acetal **12** with aryl-norbornyl-palladacycle (ANP) **C** (Fig. 4). To mitigate the tendency of nucleophilic substitution of acetal **12**,  $\text{PdCl}_2$  was used instead of  $\text{Pd}(\text{OAc})_2$  as a catalyst (entry 5). Although the nucleophilic substitution of acetal **12** is inevitable, the yield of nucleophilic substitution product **22** is slightly reduced. Subsequently, the dosage of KO<sub>2</sub>Piv and delayed addition time were screened to promote the oxidative addition of **12** with ANP **C** (entries 6-10). It was found that the reaction proceeded more efficiently with 1.8 equivalents KO<sub>2</sub>Piv when a 60 s delay was implemented for the addition (entry 7). Next, a few other ligands were tested; however, no improved results were obtained (entries 11-14). In the screening of solvents (entries 15-19), the optimal result was achieved using a mixed solvent of DMF and PhMe in a 1:1 ratio (entry 18). Notably, on a hundred-milligram scale, compound **10a** was obtained in 42% yield, and the by-product **20a**

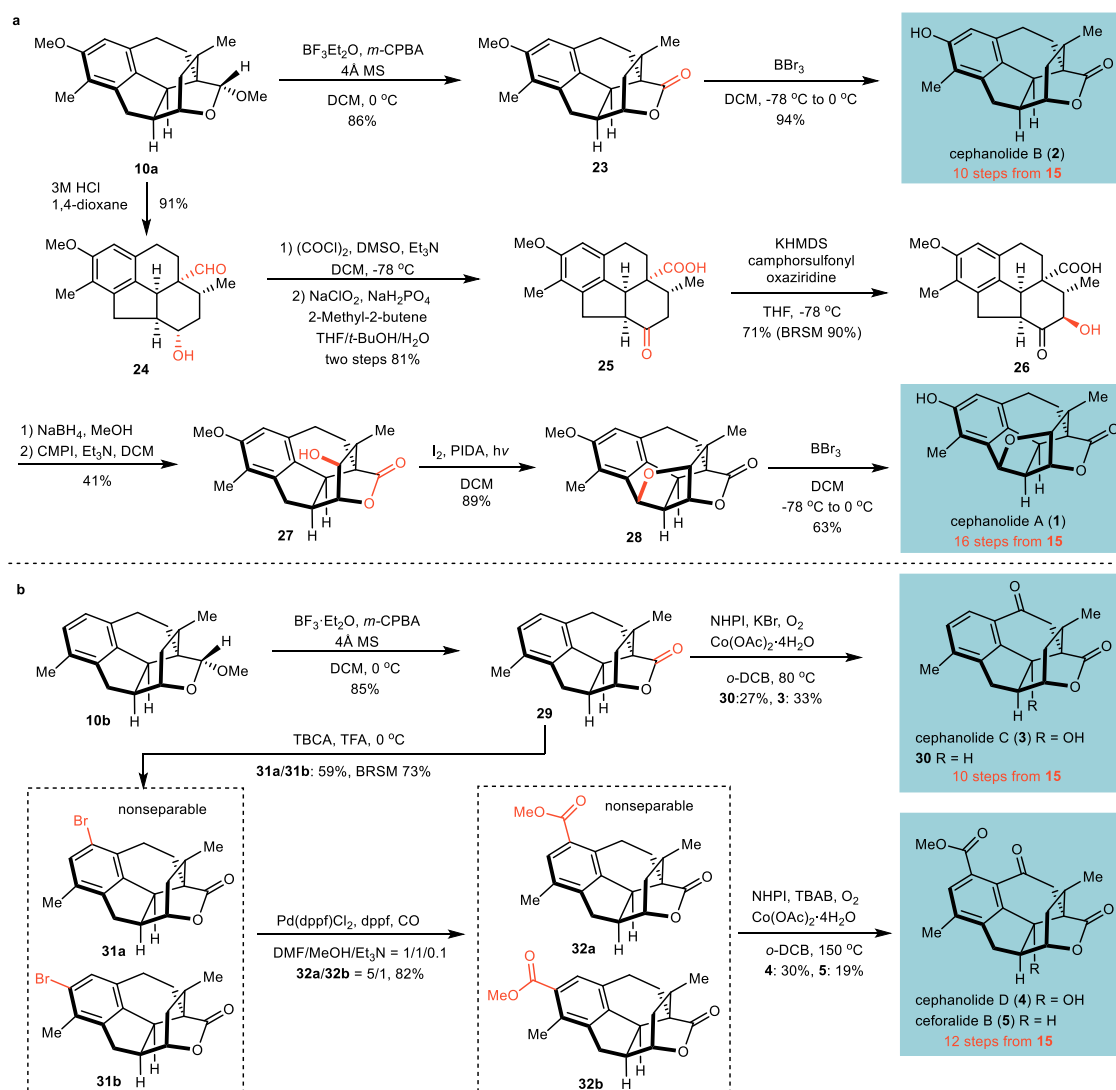


**Fig. 5 | Total Synthesis of Benzenoid Cephalotane-type Diterpenoids. a** Total Synthesis of Cephanolides A-B (**1-2**). **b** Total Synthesis of Cephanolides C-D (**3-4**) and Ceforalide B (**5**). *m*-CPBA = *m*-chloroperbenzoic acid, 4 Å MS = 4 Å molecular sieves, DCM = dichloromethane, DMSO = dimethyl sulfoxide, THF = tetrahydrofuran, KHMDS = potassium bis(trimethylsilyl)amide, BRSM = based on recovered starting

material, CMPI = 2-chloro-1-methylpyridinium iodide, PIDA = phenyliodine(III) diacetate, NHPI = N-hydroxyphthalimide, *o*-DCB = *o*-dichlorobenzene, TBCA = tetrabromocinnamic acid, dppf = 1,1'-bis(diphenylphosphino)ferrocene, DMF = *N,N*-dimethylformamide, TBAB = tetrabutylammonium bromide.



was not observed under these conditions (entry 20). Compound **10b** was obtained when **11b** reacted with acetal **12**, with a delay in the time of adding KO<sub>2</sub>Piv (entry 21). It is worth mentioning that the nucleophilic substitution compounds **21** and **22** could be reconverted to compound **12** by reduction and bromination (see Supplementary Information).

### Total synthesis of cephanolides A-D and ceforalide B

After obtaining the key compounds **10a** and **10b**, benzenoid cephalotane-type diterpenoids were synthesized through late-stage modification. Consequently, **10a** was oxidized using BF<sub>3</sub>·Et<sub>2</sub>O and *m*-CPBA to produce lactone **23**, which was subsequently deprotected with BBr<sub>3</sub> to yield cephanolide B (**2**)<sup>9,15,16</sup> (Fig. 5a). For the synthesis of cephanolide A (**1**), compound **10a** was hydrolyzed in the presence of 3 M HCl (aq.)<sup>65</sup> resulting in compound **24**. The structure of **24** was confirmed by X-ray crystallographic analysis (see Supplementary Information). Compound **24** underwent Swern oxidation and Pinnick oxidation to yield compound **25**. The Davis oxaziridine has been demonstrated to be efficacious in introducing a hydroxyl group at the C3 position<sup>17</sup>, resulting in compound **26** with 71% yield. The carbonyl of compound **26** was reduced by sodium borohydride and then underwent lactonization to give lactone **27** in the presence of Mukaiyama reagent. Lactone **27** was subjected to Suárez oxidation<sup>12,14,17,66</sup> to form the tetrahydrofuran ring of compound **28**, followed by the removal of the protective group with BBr<sub>3</sub> to yield cephanolide A (**1**). From compound **10b**, three additional benzenoid cephalotane-type diterpenoids were synthesized (Fig. 5b). Compound **10b** was oxidized to produce lactone **29**, which was then converted to cephanolide C (**3**) using the NHPI/Co(OAc)<sub>2</sub>-catalyzed oxidation as reported by Hu<sup>16</sup>. To efficiently introduce a methyl ester group in the late stage, the selective bromination at the C15 position was attempted. The expected compound **31a** was obtained in a modest yield using TBCA/TFA<sup>67</sup>, along with a small amount of non-separable C13 brominated by-product **31b**. Finally, the Pd-catalyzed methoxycarbonylation<sup>12,17</sup> resulted in compounds **32a** and **32b**, which were further oxidized to cephanolide D (**4**) and ceforalide B (**5**) via NHPI/Co(OAc)<sub>2</sub>-catalyzed oxidation.

### Discussion

In summary, we have developed a cascade C(sp<sup>2</sup>)-H and C(sp<sup>3</sup>)-H activation strategy to efficiently access the characteristic and synthetically challenging 6/6/6/5 tetracyclic skeleton of the benzenoid cephalotane-type diterpenoids, which was used to complete a short total synthesis of cephanolide B (**2**). A late-stage modification and divergent strategy were employed to complete the syntheses of four additional benzenoid cephalotane-type diterpenoids. The key feature of the cascade C(sp<sup>2</sup>) & C(sp<sup>3</sup>)-H activation reaction is the construction of three C-C bonds (two C(sp<sup>2</sup>)-C(sp<sup>3</sup>) bonds and a C(sp<sup>3</sup>)-C(sp<sup>3</sup>) bond) and two chiral centers accurately in one step via palladium/NBE-cocatalysis. Analogous strategies may prove effective in the preparation of various natural products. This encourages us to further investigate the synthesis of natural products through cascade C(sp<sup>2</sup>) & C(sp<sup>3</sup>)-H activation.

### Methods

#### Cascade C(sp<sup>2</sup>) & C(sp<sup>3</sup>)-H activation

In a 50 mL round-bottom flask, **11a** (182.0 mg, 0.9 mmol), PdCl<sub>2</sub> (32.0 mg, 20 mol%), tri(2-furyl)phosphine (83.6 mg, 40 mol%), Cs<sub>2</sub>CO<sub>3</sub> (880.0 mg, 2.7 mmol) were added and charged with argon more than three times (The flask was plugged with rubber plugs and sealed with a parafilm). Then, 5.5 mL DMF was injected into the flask via plastic syringes. The resulting light-yellow suspension was stirred vigorously at room temperature for 15 min. Norbornene (339.0 mg, 3.6 mmol) and compound **12** (353.0 mg, 1.35 mmol) were dissolved in 5.5 mL DMF, and the mixture was injected into the tube via plastic syringes.

Subsequently, the reaction tube was placed in an oil bath at 120 °C, stirred for 2 min, and then a suspension of potassium pivalate (11.0 mL in toluene) was added over 50 s. After the reaction was completed (4 h), the flask was cooled to room temperature and filtered to remove the solid residue. The filtrate is concentrated under reduced pressure, and the residue is purified by silica gel column chromatography (petroleum ether/ethyl acetate = 50/1 to 10/1) to afford compound **10a** (119.1 mg, 42%, white solid) and compound **22** (244.5 mg, 64%, colorless oil).

### Data availability

The data generated during this study are included in this article and the Supplementary Information. The X-ray crystallographic coordinates for structures reported in this study have been deposited at the Cambridge Crystallographic Data Center (CCDC), under deposition numbers 2353280 (24). These data can be obtained free of charge from The Cambridge Crystallographic Data Center via [www.ccdc.cam.ac.uk/data\\_request/cif](http://www.ccdc.cam.ac.uk/data_request/cif). Details about materials and methods, experimental procedures, characterization data, and NMR spectra are available in the Supplementary Information. All data are available from the corresponding author upon request.

### References

- Jiang, C. Y. et al. Progress in structure, synthesis and biological activity of natural cephalotane diterpenoids. *Phytochemistry* **192**, 112939 (2021).
- Ge, Z. P. et al. Cephalotane-type norditerpenoids from *Cephalotaxus fortunei* var. *alpina*. *Chin. J. Chem.* **40**, 1177–1184 (2022).
- Ge, Z.-P. et al. Cephalotane-type C20 diterpenoids from *Cephalotaxus fortunei* var. *alpina*. *Org. Biomol. Chem.* **20**, 9000–9009 (2022).
- Ge, Z.-P. et al. Highly modified cephalotane-type diterpenoids from *Cephalotaxus fortunei* var. *alpina* and *C. sinensis*. *ChemRxiv*. <https://doi.org/10.26434/chemrxiv-2023-8v6dr-v2> (2023).
- Jiang, C. et al. Diterpenolignans and cephalotane diterpenoids from *Cephalotaxus oliveri* mast. with antitumor activity. *Phytochemistry* **217**, 113924 (2024).
- Ge, Z.-P. et al. Highly modified cephalotane-type diterpenoids from *Cephalotaxus fortunei* var. *alpina* and *C. sinensis*. *Phytochemistry* **221**, 114038 (2024).
- Fan, Y.-Y. et al. Cephanolides A–J, cephalotane-type diterpenoids from *Cephalotaxus sinensis*. *J. Nat. Prod.* **80**, 3159–3166 (2017).
- Zhao, J.-X., Ge, Z.-P. & Yue, J.-M. Cephalotane diterpenoids: structural diversity, biological activity, biosynthetic proposal, and chemical synthesis. *Nat. Prod. Rep.* **41**, 1152–1179 (2024).
- Xu, L., Wang, C., Gao, Z. & Zhao, Y.-M. Total synthesis of (±)-cephanolides B and C via a palladium-catalyzed cascade cyclization and late-stage sp<sup>3</sup> C–H bond oxidation. *J. Am. Chem. Soc.* **140**, 5653–5658 (2018).
- Zhang, H., He, H. & Gao, S. Asymmetric total synthesis of cephanolide A. *Angew. Chem. Int. Ed.* **59**, 20417–20422 (2020).
- Zhang, H., He, H. & Gao, S. Asymmetric total synthesis of cephanolide B. *Org. Chem. Front.* **8**, 555–559 (2021).
- Haider, M., Sennari, G., Eggert, A. & Sarpong, R. Total synthesis of the cephalotaxus norditerpenoids (±)-cephanolides A–D. *J. Am. Chem. Soc.* **143**, 2710–2715 (2021).
- Sennari, G. et al. Unified total syntheses of benzenoid cephalotane-type norditerpenoids: cephanolides and ceforalides. *J. Am. Chem. Soc.* **144**, 19173–19185 (2022).
- Lu, Y., Xu, M. M., Zhang, Z. M., Zhang, J. & Cai, Q. Catalytic asymmetric inverse-electron-demand Diels–Alder reactions of 2-pyrone with indenones: total syntheses of cephanolides A and B. *Angew. Chem. Int. Ed.* **60**, 26610–26615 (2021).
- Li, A., He, Z., Liu, B., Yang, Z. & Zhang, Z. Stereoselective synthesis of (±)-cephanolide B. *Org. Lett.* **23**, 9237–9240 (2021).

16. Sun, Z. et al. Total synthesis of (–)-ceforalide B and (–)-cephanolides B–D. *Org. Lett.* **24**, 7507–7511 (2022).
17. Qing, Z., Mao, P., Wang, T. & Zhai, H. Asymmetric total syntheses of cephalotane-type diterpenoids cephanolides A–D. *J. Am. Chem. Soc.* **144**, 10640–10646 (2022).
18. Shao, H. et al. Bioinspired total synthesis of *Cephalotaxus* diterpenoids and their structural analogues. *Angew. Chem. Int. Ed.* **63**, e202402931 (2024).
19. Wiesler, S. et al. Late-stage benzenoid-to-troponoid skeletal modification of the cephalotanes exemplified by the total synthesis of harringtonolide. *Nat. Commun.* **15**, 4125 (2024).
20. Chen, P., Chen, L., Lin, H. & Jia, Y. Total synthesis of (+)-mannolide B. *J. Am. Chem. Soc.* **147**, 636–643 (2025).
21. Gan, X.-C. et al. Unified total synthesis of benzenoid and troponoid *Cephalotaxus* diterpenoids enabled by regiocontrolled phenol-to-troponone ring expansion. *JACS Au*. <https://doi.org/10.1021/jacsau.4c01067>.
22. Arndtsen, B. A., Bergman, R. G., Mobley, T. A. & Peterson, T. H. Selective intermolecular carbon–hydrogen bond activation by synthetic metal complexes in homogeneous solution. *Acc. Chem. Res.* **28**, 154–162 (1995).
23. Chai, Z. G. Heterogeneous photocatalytic strategies for C(sp<sup>3</sup>) activation. *Angew. Chem. Int. Ed.* **63**, e202316444 (2024).
24. Jiang, Y., Fan, Y., Li, S. & Tang, Z. Photocatalytic methane conversion: insight into the mechanism of C(sp<sup>3</sup>)-H bond activation. *CCS Chem.* **5**, 30–54 (2023).
25. Saha, D., Das, P., Biswas, P. & Guin, J. Synthesis of phenolic compounds via palladium catalyzed C–H functionalization of arenes. *Chem.-Asian J.* **14**, 4534–4548 (2019).
26. Tao, P. & Jia, Y. C–H bond activation in the total syntheses of natural products. *Sci. Chin. Chem.* **59**, 1109–1125 (2016).
27. Sinha, S. K., Zanoni, G. & Maiti, D. Natural product synthesis by C–H activation. *Asian J. Org. Chem.* **7**, 1178–1192 (2018).
28. Abrams, D. J., Provencher, P. A. & Sorensen, E. J. Recent applications of C–H functionalization in complex natural product synthesis. *Chem. Soc. Rev.* **47**, 8925–8967 (2018).
29. Karimov, R. R. & Hartwig, J. F. Transition-metal-catalyzed selective functionalization of C(sp<sup>3</sup>)-H bonds in natural products. *Angew. Chem. Int. Ed.* **57**, 4234–4241 (2018).
30. Baudoin, O. Multiple catalytic C–H bond functionalization for natural product synthesis. *Angew. Chem. Int. Ed.* **59**, 17798–17809 (2020).
31. Lam, N. Y. S., Wu, K. & Yu, J.-Q. Advancing the logic of chemical synthesis: C–H activation as strategic and tactical disconnections for C–C bond construction. *Angew. Chem. Int. Ed.* **60**, 15767–15790 (2021).
32. Catellani, M., Frignani, F. & Rangoni, A. A complex catalytic cycle leading to a regioselective synthesis of o,o'-disubstituted vinylarenes. *Angew. Chem. Int. Ed.* **36**, 119–122 (1997).
33. Della Ca', N., Fontana, M., Motti, E. & Catellani, M. Pd/Norbornene: a winning combination for selective aromatic functionalization via C–H bond activation. *Acc. Chem. Res.* **49**, 1389–1400 (2016).
34. Lautens, M. & Piguel, S. A new route to fused aromatic compounds by using a palladium-catalyzed alkylation - alkenylation sequence. *Angew. Chem. Int. Ed.* **39**, 1045–1046 (2000).
35. Gericke, K. M., Chai, D. I., Bieler, N. & Lautens, M. The norbornene shuttle: multicomponent domino synthesis of tetrasubstituted helical alkenes through multiple C–H functionalization. *Angew. Chem. Int. Ed.* **48**, 1447–1451 (2009).
36. Ye, J. & Lautens, M. Palladium-catalysed norbornene-mediated C–H functionalization of arenes. *Nat. Chem.* **7**, 863–870 (2015).
37. Wang, J. & Dong, G. Palladium/norbornene cooperative catalysis. *Chem. Rev.* **119**, 7478–7528 (2019).
38. Wang, J., Dong, Z., Yang, C. & Dong, G. Modular and regioselective synthesis of all-carbon tetrasubstituted olefins enabled by an alkenyl catellani reaction. *Nat. Chem.* **11**, 1106–1112 (2019).
39. Li, R. & Dong, G. Structurally modified norbornenes: a key factor to modulate reaction selectivity in the palladium/norbornene cooperative catalysis. *J. Am. Chem. Soc.* **142**, 17859–17875 (2020).
40. Cheng, H., Chen, S., Chen, R. & Zhou, Q. Palladium(II)-initiated catellani-type reactions. *Angew. Chem. Int. Ed.* **58**, 5832–5844 (2019).
41. Dong, S. & Luan, X. Catellani reaction: an enabling technology for vicinal functionalization of aryl halides by palladium(0)/norbornene cooperative catalysis. *Chin. J. Chem.* **39**, 1690–1705 (2021).
42. Cheng, H.-G., Jia, S. & Zhou, Q. Benzo-fused-ring toolbox based on palladium/norbornene cooperative catalysis: methodology development and applications in natural product synthesis. *Acc. Chem. Res.* **56**, 573–591 (2023).
43. Sui, X., Zhu, R., Li, G., Ma, X. & Gu, Z. Pd-catalyzed chemoselective catellani ortho-arylation of iodopyrroles: rapid total synthesis of rhazinal. *J. Am. Chem. Soc.* **135**, 9318–9321 (2013).
44. Weinstabl, H., Suhartono, M., Qureshi, Z. & Lautens, M. Total synthesis of (+)-linoxepin by utilizing the catellani reaction. *Angew. Chem. Int. Ed.* **52**, 5305–5308 (2013).
45. Jiang, S. Z. et al. Iridium-catalyzed enantioselective indole cyclization: application to the total synthesis and absolute stereochemical assignment of (–)-aspidophylline A. *Angew. Chem. Int. Ed.* **55**, 4044–4048 (2016).
46. Liu, F., Dong, Z., Wang, J. & Dong, G. Palladium/norbornene-catalyzed indenone synthesis from simple aryl iodides: concise syntheses of pauciflorol F and acredinone A. *Angew. Chem. Int. Ed.* **58**, 2144–2148 (2019).
47. Zhao, K., Xu, S., Pan, C., Sui, X. & Gu, Z. Catalytically asymmetric Pd/norbornene catalysis: enantioselective synthesis of (+)-rhazinal, (+)-rhazinilam, and (+)-kopsiunnanine C1–3. *Org. Lett.* **18**, 3782–3785 (2016).
48. Gao, S., Qian, G., Tang, H., Yang, Z. & Zhou, Q. Three-step total synthesis of ramelteon via a catellani strategy. *ChemCatChem* **11**, 5762–5765 (2019).
49. Cheng, H.-G. et al. A concise total synthesis of (–)-berkelic acid. *Angew. Chem. Int. Ed.* **60**, 5141–5146 (2021).
50. Zhao, P., Guo, Y. & Luan, X. Total synthesis of dalesconol A by Pd(0)/norbornene-catalyzed three-fold domino reaction and Pd(II)-catalyzed trihydroxylation. *J. Am. Chem. Soc.* **143**, 21270–21274 (2021).
51. Bai, M., Jia, S., Zhang, J., Cheng, H. G., Cong, H., Liu, S., Huang, Z., Huang, Y., Chen, X. & Zhou, Q. A modular approach for diversity-oriented synthesis of 1,3-trans-disubstituted tetrahydroisoquinolines: seven-step asymmetric synthesis of michellamines B and C. *Angew. Chem. Int. Ed.* **61**, e202205245 (2022).
52. Richardson, A. D., Vogel, T. R., Traficante, E. F., Glover, K. J. & Schindler, C. S. Total synthesis of (+)-cochlearol B by an approach based on a catellani reaction and visible-light-enabled [2+2] cycloaddition. *Angew. Chem. Int. Ed.* **61**, e202201213 (2022).
53. Yang, Z. et al. Eight-step asymmetric synthesis of (–)-berkelic acid. *Synthesis* **54**, 4691–4702 (2022).
54. Jia, S. et al. Quick assembly of 1-alkylidenyl-tetrahydroisoquinolines via a catellani reaction/NBS-mediated cyclization sequence and synthetic applications. *Sci. China Chem.* **66**, 3136–3140 (2023).
55. Catellani, M., Mottia, E. & Ghellib, S. Intramolecular benzylic C–H activation: palladium-catalyzed synthesis of hexahydromethanofluorenes. *Chem. Commun.* **2003**, 2004 (2000).
56. Catellani, M., Cugini, F. & Tiefenthaler, D. New pathways of site selective aromatic alkylation of palladium complexes: fragmentation to arenes vs. ring closure to hexahydromethanofluorenes or phenanthrenes. *Can. J. Chem.* **79**, 742–751 (2001).

57. Rouquet, G. & Chatani, N. Catalytic functionalization of C(sp<sup>2</sup>)-H and C(sp<sup>3</sup>)-H bonds by using bidentate directing groups. *Angew. Chem. Int. Ed.* **52**, 11726–11743 (2013).
58. He, J., Wasa, M., Chan, K. S. L., Shao, Q. & Yu, J.-Q. Palladium-catalyzed transformations of alkyl C–H bonds. *Chem. Rev.* **117**, 8754–8786 (2016).
59. Yu, X. et al. Enantioselective total syntheses of various amphilectane and serrulatane diterpenoids via cope rearrangements. *J. Am. Chem. Soc.* **138**, 6261–6270 (2016).
60. Xu, Z., Wang, Q. & Zhu, J. Total syntheses of (–)-mersicarpine, (–)-scholarisine G, (+)-melodinine E, (–)-leuconoxine, (–)-leuconolam, (–)-leuconodine A, (+)-leuconodine F, and (–)-leuconodine C: self-induced diastereomeric anisochronism (SIDA) phenomenon for scholarisine G and leuconodines A and C. *J. Am. Chem. Soc.* **137**, 6712–6724 (2015).
61. Nickon, A. & Werstiuk, NickH. 7-endo radical cyclizations catalyzed by titanocene(III) straightforward synthesis of terpenoids with seven-membered carbocycles. *J. Am. Chem. Soc.* **127**, 14911–14921 (2005).
62. Du, W., Gu, Q., Li, Z. & Yang, D. Palladium(II)-catalyzed intramolecular tandem aminoalkylation via divergent C(sp<sup>3</sup>)-H functionalization. *J. Am. Chem. Soc.* **137**, 1130–1135 (2015).
63. Chung, D. S. et al. Palladium-catalyzed divergent cyclopropanation by regioselective solvent-driven C(sp<sup>3</sup>)-H bond activation. *Angew. Chem. Int. Ed.* **57**, 15460–15464 (2018).
64. Clemenceau, A., Thesmar, P., Gicquel, M., Le Flohic, A. & Baudoin, O. Direct synthesis of cyclopropanes from gem-dialkyl groups through double C–H activation. *J. Am. Chem. Soc.* **142**, 15355–15361 (2020).
65. Asaba, T., Katoh, Y., Urabe, D. & Inoue, M. Total synthesis of crotophorbolone. *Angew. Chem. Int. Ed.* **54**, 14457–14461 (2015).
66. Concepción, J. I., Francisco, C. G., Hernández, R., Salazar, J. A. & Suárez, E. Intramolecular hydrogen abstraction. Iodosobenzene diacetate, an efficient and convenient reagent for alkoxy radical generation. *Tetrahedron Lett.* **25**, 1953–1956 (1984).
67. Tomanik, M. & Yu, J.-Q. Palladium-catalyzed stitching of 1,3-C(sp<sup>3</sup>)-H bonds with dihaloarenes: short synthesis of (±)-echinolactone D. *J. Am. Chem. Soc.* **145**, 17919–17925 (2023).

## Acknowledgements

We gratefully acknowledge financial support from the National Natural Science Foundation of China (Grants 22271129 and 21971096 Z. X. Xie) and the Science and Technology Major Program of Gansu Province of China (22ZD6FA006, 23ZDFA015, and 24ZD13FA017 Z. X. Xie).

## Author contributions

Z.X. Xie conceived the projects. X.X. Li, Z.X. Lu, S.C. Liu, M.Y. Sun, and S.F. Duan performed the experiments under the supervision of Z.X. Xie. Z.X. Xie and X.X. Li wrote the manuscript with the feedback of all other authors.

## Competing interests

The authors declare no competing interests.

## Additional information

**Supplementary information** The online version contains supplementary material available at <https://doi.org/10.1038/s41467-025-59816-w>.

**Correspondence** and requests for materials should be addressed to Zhixiang Xie.

**Peer review information** *Nature Communications* thanks the anonymous reviewer(s) for their contribution to the peer review of this work. A peer review file is available.

**Reprints and permissions information** is available at <http://www.nature.com/reprints>

**Publisher's note** Springer Nature remains neutral with regard to jurisdictional claims in published maps and institutional affiliations.

**Open Access** This article is licensed under a Creative Commons Attribution-NonCommercial-NoDerivatives 4.0 International License, which permits any non-commercial use, sharing, distribution and reproduction in any medium or format, as long as you give appropriate credit to the original author(s) and the source, provide a link to the Creative Commons licence, and indicate if you modified the licensed material. You do not have permission under this licence to share adapted material derived from this article or parts of it. The images or other third party material in this article are included in the article's Creative Commons licence, unless indicated otherwise in a credit line to the material. If material is not included in the article's Creative Commons licence and your intended use is not permitted by statutory regulation or exceeds the permitted use, you will need to obtain permission directly from the copyright holder. To view a copy of this licence, visit <http://creativecommons.org/licenses/by-nc-nd/4.0/>.

© The Author(s) 2025